

Cationic Gemini Surfactants as Novel Corrosion Inhibitor for Mild Steel in 1M HCl

M. Mobin*, Sheerin Masroor

Corrosion Research Laboratory, Department of Applied Chemistry, Faculty of Engineering and Technology, Aligarh Muslim University, Aligarh (U.P) 202002-India

*E-mail: drmmobin@hotmail.com

Received: 19 June 2012 / Accepted: 13 July 2012 / Published: 1 August 2012

The corrosion inhibition characteristics of synthesized cationic gemini surfactants of the series, 14-n-14 (n=4,6) namely, 1,4-bis(N-tetradecyl-N,N dimethyl ammonium) butane dibromide (14-4-14) and 1,6-bis(N-tetradecyl-N,N dimethyl ammonium) hexane dibromide (14-6-14), on the mild steel in 1 M HCl solution as a function of inhibitor concentration (2.5×10^{-5} - 2.5×10^{-7} M) and the solution temperature (30-60 °C) was studied. The synthesized surfactants were characterized by Nuclear Magnetic Resonance (NMR) spectroscopy. The inhibition efficiency (IE) of the inhibitors was investigated by weight loss measurements, solvent analysis of iron ions, potentiodynamic polarization measurements and electrochemical impedance spectroscopy (EIS). The surface analysis of the corroded steel samples in absence and presence of surfactants was also evaluated by Scanning Electron Microscopy (SEM) and Atomic Force Microscopy (AFM). The %IE of the inhibitors increased with increase in surfactant concentration and temperature; the %IE being in the range 70-98%. The adsorption of gemini surfactants on the steel surface obey Langmuir adsorption isotherm from the fit of the experimental data of all concentration and temperature studied. The associated activation energy of corrosion (E_a) and other thermodynamic parameters such as enthalpy of adsorption (ΔH), entropy of adsorption (ΔS), adsorption equilibrium constant (K_{ads}) and standard free energy of adsorption (ΔG_{ads}) were calculated to elaborate the mechanism of corrosion inhibition.

Keywords: Cationic Gemini surfactant, Corrosion inhibitor, potentiodynamic polarization, ac impedance, SEM, AFM.

1. INTRODUCTION

The corrosion of mild steel in acidic solutions has been a subject of both academic and industrial concern and has received considerable attention during the last few decades. Among the

acids, hydrochloric acid is widely used for removal of rust and scales in several industrial operations. However, hydrochloric acid is a strong corrosive agent and its corrosivity needs to be controlled by using appropriate corrosion inhibitor. There are various organic compounds which tend to reduce the corrosivity of acid solution [1-5]. Most of the effective organic inhibitors used contain heteroatom (e.g., O, N, and S) and multiple bonds in their molecules through which they are adsorbed on the metal surface [6-12]. The adsorption may occur via (i) electrostatic attraction between the charged inhibitor molecules and the charged metal, (ii) interaction between the electron pairs in the inhibitor molecule and the metal, (iii) π electron interaction with the metal and (iv) a combination of all [13,14].

Surfactants, because of their remarkable ability to influence the properties of surfaces and interfaces, have been effectively exploited as corrosion inhibitor in acidic medium [15-25]. Surfactants are amphiphilic molecules containing one hydrophilic (head) and other hydrophobic (tail) parts; this favors the adsorption process at metallic surfaces. The hydrophilic part of the surfactant may be positive, negative, neutral or zwitterionic and the hydrophobic part consists of one or more hydrocarbon chains, usually with 6-22 carbon atoms. The adsorption process depends upon the structure and concentration of surfactant molecules in the contacting medium [26]. The adsorbed molecules form a monolayer or bilayer, hemimicelles or admicelles and prevent the acids to attack the surface, and thus reduce the corrosion.

Gemini or dimeric surfactants (GS) are a new class of surfactant developed in recent years which have attracted great attention in corrosion inhibition [27-30]. A gemini surfactant consists of two conventional surfactant molecules chemically bonded together by a spacer. The two terminal hydrocarbon tails can be short or long; the two polar head groups can be cationic, anionic or nonionic; the spacer can be short or long, flexible or rigid. The GS need to be symmetrically disposed about the center of the spacer, can self assemble at much lower concentrations and are superior in the surface activity as compared to conventional surfactants. These surfactants have very low critical micelle concentration (CMC) and have high solubilising capacity than the corresponding conventional surfactants. The adsorption mechanism of GS on steel surface is quite different and more complicated from that of conventional single chained surfactants. Like conventional surfactants, in case of GS also multilayer may form at surfactant concentration above CMC. However, before multilayer may form three different situations may be visualized [31]. In first situation two hydrophilic ionic groups of GS may be adsorbed on the metal surface. In second situation one hydrophilic ionic group is adsorbed on the surface whereas the second hydrophilic ionic group is free in the solution phase. Thirdly, both the situation may coexist. At lower concentration of the GS the main adsorption mechanism is governed by the first situation. At high concentration adsorption mechanism is governed by the second situation but the third situation appears to be more reasonable because of the interaction between the molecules of GS. The present work is aimed to study the corrosion inhibition behavior of two novel GS namely, 1,4-bis(N-tetradecyl-N,N dimethyl ammonium) butane dibromide (14-4-14) and 1,6-bis(N-tetradecyl-N,N dimethyl ammonium) hexane dibromide (14-6-14), on mild steel in 1M HCl in the temperature range of 30-60 °C.

2. EXPERIMENTAL PROCEDURE

2.1. Material preparation

Mild steel samples having composition 0.034% C, 0.176% Mn, 0.0103% P, 0.059% Pb, 0.014% Al, 0.034% V and balance Fe were used for corrosion inhibition studies. The mild steel coupons of size (2.0×2.0×0.04cm) were machined with a series of emery papers, followed by rinsing in acetone and double distilled water (DDW) and then dried in air. Prior to any experiment, the substrates were treated as described and freshly used with no further storage. The solution of 1M HCl was prepared by using AR grade HCl (Qualigens) and DDW.

2.2. Synthesis and characterisation of gemini surfactants

The GS studied were synthesized in laboratory following an identical synthetic route described earlier [32,33]. The synthesized products were characterized by NMR. ¹H NMR spectra of the compounds were obtained in CDCl₃ using a BRUKER DRX-300 NMR spectrometer operated at 300.13 MHz. The name and molecular structures of the synthesized compounds are given in Table 1.

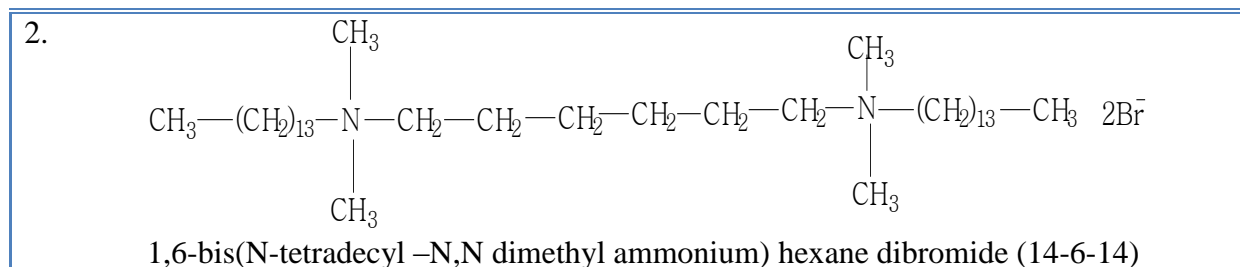
2.3. Weight loss measurements

The weight loss experiments were carried out in a thermostated water bath for duration of 6h as per ASTM designation G1-90. The freshly prepared specimens were suspended in 250 ml beakers containing 200 ml of test solutions maintained at 30-60 °C. The samples were immersed in triplicate and average corrosion rate was calculated. The uncertainty for three replicate measurements was less than 5%. The corrosion rate was calculated using equation:

$$\text{Corrosion rate (CR) (mpy)} = \frac{534 W}{\rho AT} \quad (1)$$

Table 1. Name and molecular structure of gemini surfactants

S. No.	Molecular structure / Name and abbreviation
1.	$\begin{array}{c} \text{CH}_3 \\ \\ \text{CH}_3 - (\text{CH}_2)_{13} - \text{N} - \text{CH}_2 - \text{CH}_2 - \text{CH}_2 - \text{CH}_2 - \text{N} - (\text{CH}_2)_{13} - \text{CH}_3 \\ \qquad \qquad \qquad \\ \text{CH}_3 \qquad \qquad \qquad \text{CH}_3 \end{array} \quad 2\text{Br}^-$ <p>1,4-bis(N-tetradecyl-N,N dimethyl ammonium) butane dibromide (14-4-14)</p>



where, W is weight loss in mg; ρ is the density of specimen in g/cm^3 ; A is the area of specimen in square inch and t is exposure time in hrs. The %IE of the surfactants was evaluated using the following equation:

$$(\%IE) = \frac{CR_o - CR_i}{CR_o} \times 100 \quad (2)$$

where, CR_o is the corrosion rate of mild steel in absence of inhibitor and CR_i is the corrosion rate of mild steel in presence of inhibitor.

2.4. Solution analysis of metal ions

The corrosion rate and IE of mild steel in absence and presence of inhibitors was also investigated from the determination of total iron ions ($\text{Fe}^{2+}/\text{Fe}^{3+}$) entered into the test solution in the course of corrosion during immersion. The analysis was performed spectrophotometrically [34, 35] using a calibration curve prepared from standard solutions. 1, 10-orthophenanthroline was used for producing the colored complex with Fe^{2+} ions. Hydroxylamine (HCl salt) was added as reducing agent before color is developed to provide a measure of total Fe ions present into the solution. The pH of the solution was adjusted to a value between 6 and 9 by adding sodium acetate buffer. The samples were immersed in triplicate and the average corrosion rate was calculated. The uncertainty for three replicate measurements was less than 5%. A double beam spectrophotometer (Model: Elico-SL-169 UV-Visible Spectrophotometer) was used for analysis of iron ions in the solutions. The corrosion rate was calculated using the following relationship:

$$\text{Corrosion rate} = \frac{m}{s \times t} [\text{gm}^{-1}\text{h}^{-1}] \quad (3)$$

where, ' m ' is the mass of corroded metal (calculated from the total iron content determined in the test solution); ' s ' is the area of the test metal in m^2 ; and ' t ' is the exposure time in hrs. The %IE of the inhibitors was calculated using the Eq. (2).

2.5. Potentiodynamic polarization measurements

The potentiodynamic polarization measurements were carried out on Micro Autolab type III potentiostat/Galvanostat (Model: μ 3AVT 70762, Netherlands) with Ag/AgCl electrode (saturated KCl) as reference and Pt wire as counter electrode. The experiments were performed by sweeping the potential between -0.25 and 0.25 V from open circuit potential at a scan rate of 0.0005 V/s. The specimen was allowed to stabilize in the electrolyte for 30 min prior to the experiment. All the experiments were done at room temperature ($30 \pm 1^\circ\text{C}$).

2.6. Electrochemical impedance (EIS) measurements

Electrochemical impedance (EIS) measurements were carried out using Ivium potentiostat/galvanostat (Model: IviumStat). All electrochemical experiments were performed in a conventional three electrode cell at 30°C , with platinum as counter electrode, Ag/AgCl as reference electrode, and mild steel as working electrode, with exposed surface of 1 cm^2 , was placed into the aggressive solution. EIS measurements were implemented at open circuit potential within frequency range of 10^{-2} Hz to 10^4 Hz with 10mV perturbation.

2.7. Scanning Electron Microscopy (SEM) and Atomic Force Microscopy (AFM) studies

The surface morphology of mild steel specimens immersed in uninhibited and inhibited acid solution was evaluated using SEM (Model: JEOL JSM- 6510LV), and AFM (model: Innova SPM, Veeco). After completion of immersion, the test specimens were thoroughly washed with DDW and dried and then subjected to SEM and AFM studies.

3. RESULTS AND DISCUSSION

3.1. Characterization of gemini surfactants

The synthesized GS were characterized using NMR technique. The ^1H NMR spectra of synthesized compounds are shown in Fig. 1. The pertinent details of NMR of the synthesized GS are as follows:

14-4-14: ^1H NMR (CDCl_3) $\delta(\text{ppm})$ 0.859-0.903 (t, 6H), 1.257-1.354 (m, 40H), 1.760 (m, 4H), 2.106 (m, 4H), 3.070 (s, 12H), 3.312-3.442 (t, 4H), 3.468 (s, 4H), 3.864 (s, 4H).

14-6-14: ^1H NMR (CDCl_3) $\delta(\text{ppm})$ 0.862-0.881 (t, 6H), 1.256-1.353 (m, 44H), 1.562 (m, 4H), 1.722 (m, 4H), 1.975 (s, 4H), 2.956 (s, 12H), 3.484-3.509 (t, 4H), 3.532-3.678 (t, 4H).

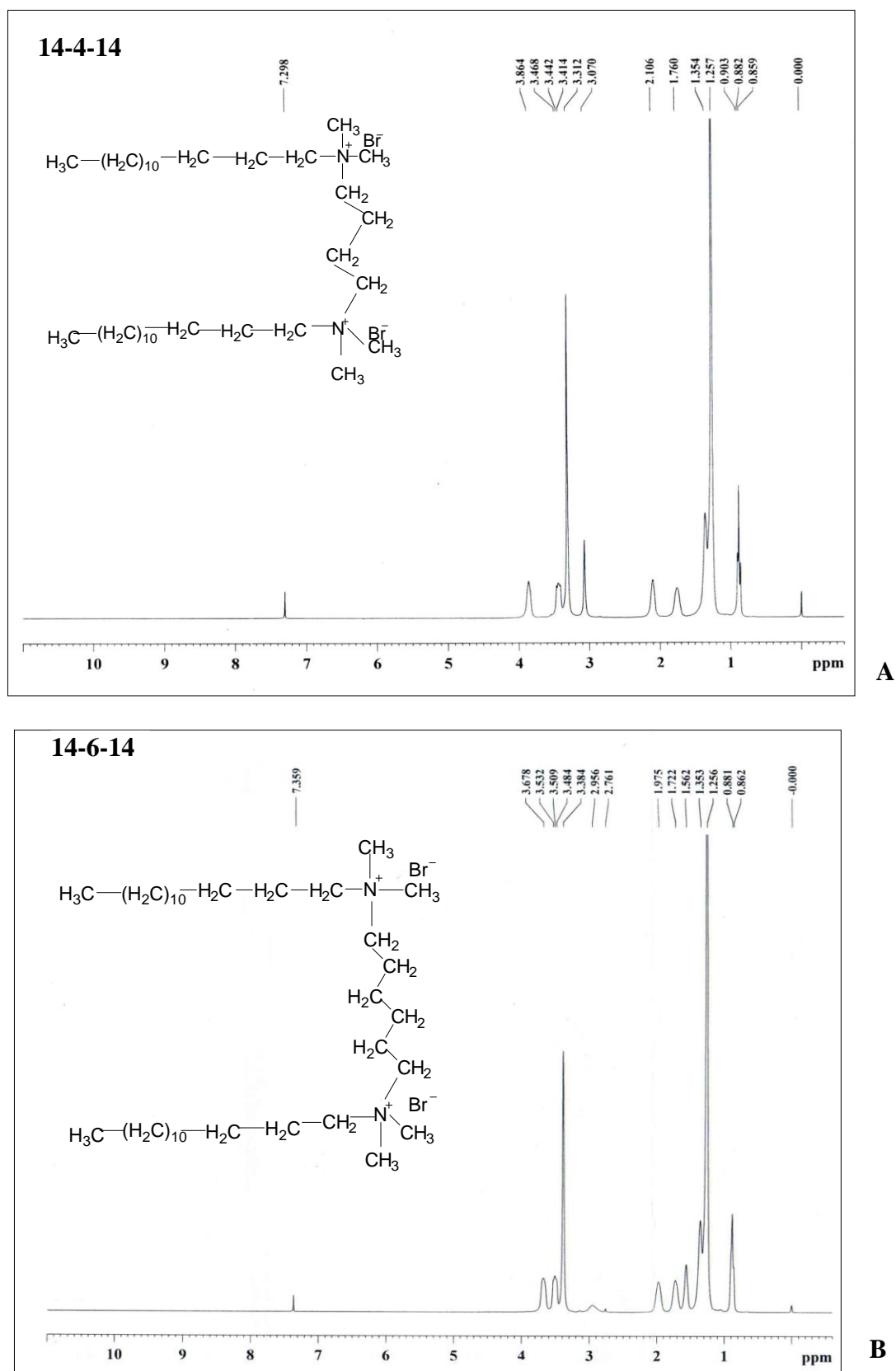


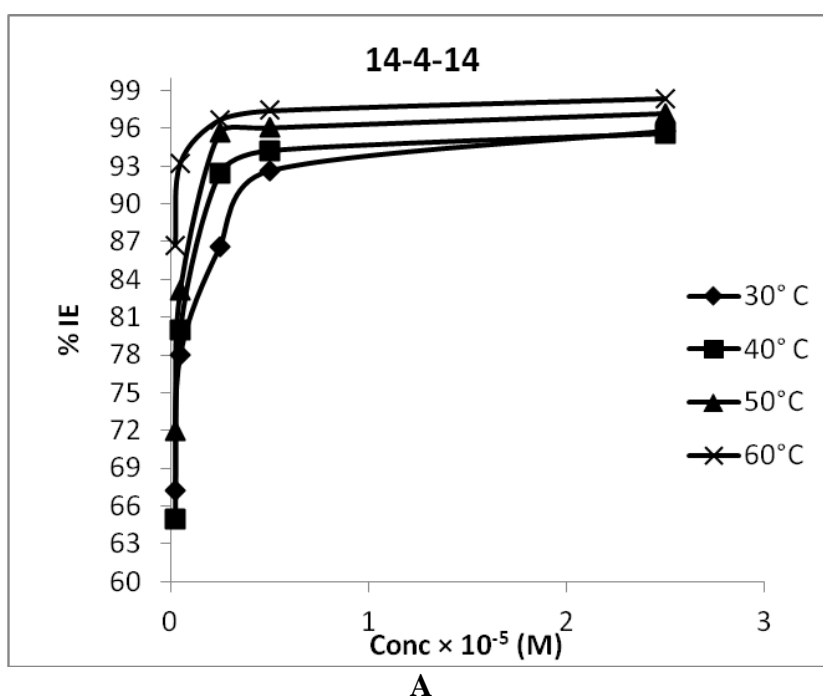
Figure 1. NMR Spectra of the synthesized gemini surfactants and their molecular structure (A) 14-4-14, (B) 14-6-14.

3.2. Weight loss measurements

The corrosion inhibition of mild steel in 1 M HCl at 30-60 °C in absence and presence of different concentrations of GS was studied using weight loss technique and the data obtained after 6 h of immersion have been recorded in Table 2.

Table 2. Corrosion parameters for mild steel in 1 M HCl in absence and presence of the GS from weight loss measurements at different temperatures

Surfactant concentration (M)	Corrosion rate (mpy)				Inhibition Efficiency (%IE)			
	30°C	40°C	50°C	60°C	30°C	40°C	50°C	60°C
Blank	639.47	938.27	2879.16	6372.85	-	-	-	-
14-4-14								
2.5×10^{-7}	209.42	328.40	663.68	828.47	67.25	65.00	72.00	86.70
5×10^{-7}	140.68	187.65	402.95	446.10	78.00	80.00	83.12	93.25
2.5×10^{-6}	83.13	75.06	101.92	191.19	86.56	92.44	95.73	96.72
5×10^{-6}	44.76	56.30	94.81	191.19	92.61	94.24	96.08	97.43
2.5×10^{-5}	25.60	41.60	71.11	127.46	95.78	95.60	97.22	98.41
14-6-14								
2.5×10^{-7}	198.24	281.48	639.98	1465.76	69.00	69.90	73.00	77.00
5×10^{-7}	159.87	262.72	521.46	1210.84	75.00	72.00	78.00	81.00
2.5×10^{-6}	147.08	253.33	260.73	446.10	77.29	73.73	88.96	92.79
5×10^{-6}	108.71	121.98	165.92	318.64	82.58	87.29	92.95	94.86
2.5×10^{-5}	57.56	84.44	130.60	191.19	90.49	91.00	94.50	97.40



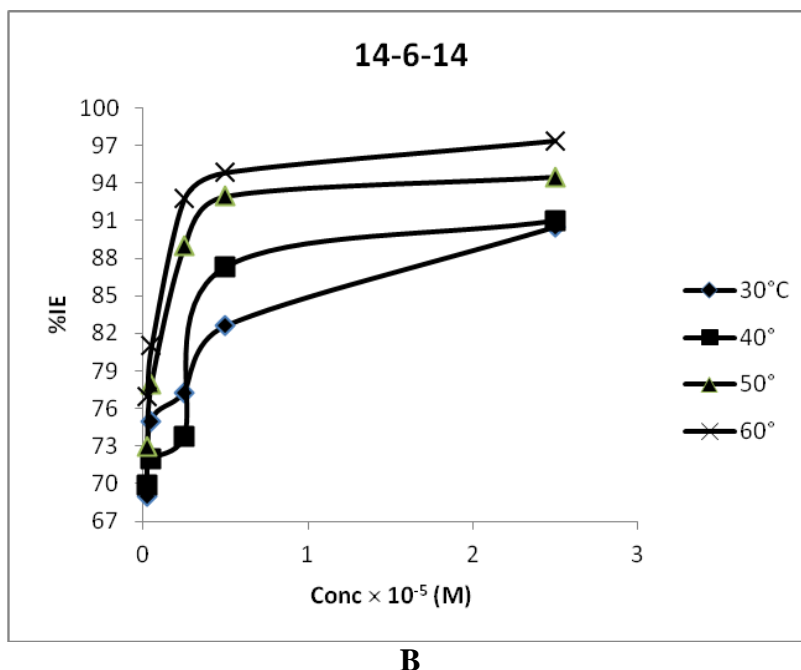


Figure 2. Plot of % IE as a function of surfactants concentrations at 30-60 °C (A) 14-4-14 and (B) 14-6-16.

The corrosion rate is reduced in presence of both the GS as compared to the free acid solution. Also the corrosion rate increased with increase in temperature at all concentrations studied. The plot of % IE as a function of surfactants concentrations at 30-60 °C reveals that at given temperature the IE increases with increase in surfactant concentrations (Fig.2). The effect of temperature on IE is quite pronounced; the IE increases with increase in temperature.

The inhibition of mild steel corrosion by GS can be explained in terms of their adsorption on the steel surface. Both the GS used during the investigation showed excellent %IE well below their CMC; the values of CMC for surfactants 14-4-14 and 14-6-14 at 30 °C being 1.2×10^{-4} and 1.4×10^{-4} M, respectively. The excellent IE of the compounds is due to high degree of surface coverage resulting from their adsorption on the steel surface. The strong adsorption in case of double chained GS can be explained on the basis of electrostatic interaction between the two ammonium groups and the cathodic sites on the steel surface. Below CMC as the surfactants concentration increases, the molecules tend to aggregate at the interface and the interfacial aggregation reduces the surface tension, thereby resulting in reduced corrosion rate. The comparison of the corrosion performance of both surfactants showed that 14-4-14 has slightly higher values of IE than 14-6-14. This may be due to the fact that though both the surfactants have same geometric length of the hydrophobic chain (C₁₄) but have different spacer length (4 and 6, respectively). A higher IE of 14-4-14 might be due to its smaller spacer size. A smaller spacer size means shorter distance between the two head groups in unit gemini molecule, thereby enhancing the charge density of head groups and favoring the adsorption of surfactant [36]. Considering the effect of temperature on inhibition behavior of GS, the IE also increases with increase in temperature. This pointed to the capability of surfactants to inhibit corrosion of steel at low and relatively high temperatures. The GS on steel surface are chemically adsorbed on to the mild steel

surface which is more favored at higher temperature due to lesser kinetic energy barrier. The effect of immersion time on the IE of the GS was also studied at 30 °C and the results are presented in Fig. 3. The IE does not appear to be significantly affected with increase in immersion period; this shows the persistency of the adsorbed surfactants film over a longer test period. The IE of the surfactants as obtained by solvent analysis of iron ions at 30 °C (Table 3) is consistent with the results of weight loss measurements.

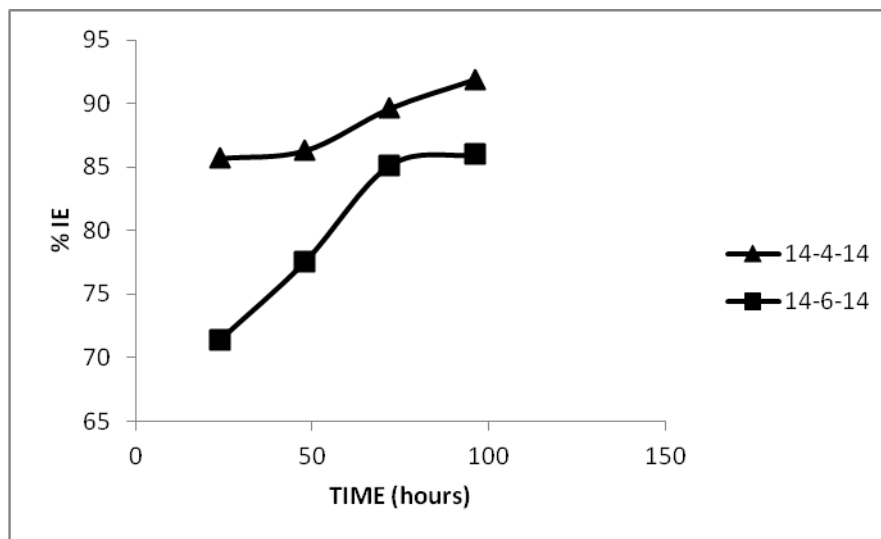


Figure 3. Variation of % IE with time.

3.3. Adsorption Isotherms

Adsorption isotherms are very important in determining the mechanism of organo-electrochemical reactions. In present study, Langmuir adsorption isotherm was found to be suitable for the experimental findings. The isotherm is described by equation:

$$\frac{C}{\theta} = \frac{1}{k} + C \quad (4)$$

where, θ is the degree of surface coverage, K is the equilibrium constant of the adsorption process and C is the surfactant concentration. The plots of C/θ versus C for mild steel corrosion in 1M HCl for surfactants 14-4-14 and 14-6-14 at temperature 30 °C is shown in Fig.4. The values of adsorption parameters deduced from the Langmuir adsorption isotherm (linear regression parameters) such as linear regression coefficient, slope and adsorptive equilibrium constants are presented in Table 4. A linear correlation of slope close to unity suggests that adsorption of surfactants on mild steel interface obeys Langmuir adsorption isotherm. The high values of K indicate that the GS are strongly adsorbed on the steel surface. The values of K for surfactant 14-4-14 is more than the surfactant 14-6-14, this implies more efficient adsorption of 14-4-14 and hence better IE. The surfactant 14-4-14 is more effective as an inhibitor for steel corrosion than that the surfactant 14-6-14.

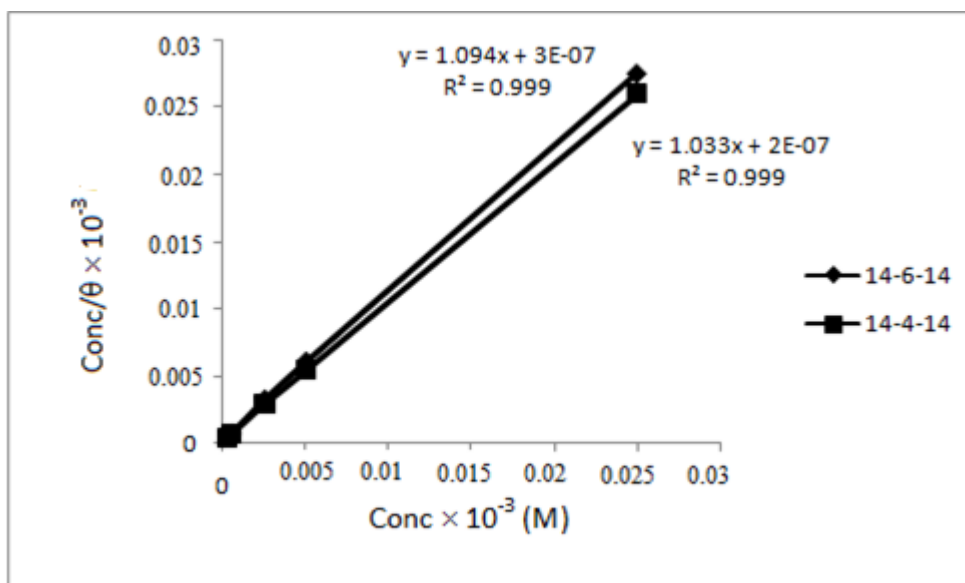


Figure 4. Langmuir adsorption isotherms for 14-4-14 and 14-6-14.

Table 3. Parameters from Langmuir adsorption isotherm, value of linear regression, slope, and K at different temperatures

Surfactants	R ²	Slope	K×10 ⁴			
			30°C	40°C	50°C	60°
14-4-14	0.999	1.003	96	76	129.33	196
14-6-14	0.999	1.094	36	40.44	76	129.33

3.4. Effect of temperature

In order to elucidate the inhibitive properties of the GS and the temperature dependence on the corrosion rates, the apparent activation energy (E_a) for the corrosion process in the absence and presence of surfactants were evaluated from Arrhenius equation given by relationship:

$$\log CR = \log A - \frac{E_a}{2.303RT} \tag{5}$$

where, CR is the corrosion rate, A is the Arrhenius constant, E_a is the apparent activation energy, R is the molar gas constant and T is the absolute temperature. The logarithm of corrosion rate (log CR) versus reciprocal of absolute temperature (1/T) for 1M HCl for blank, 14-4-14 and 14-6-14, is presented in Fig. 5. The values of E_a obtained from the slope of the linear plot are presented in Table 5. The other kinetic parameters such as enthalpy of adsorption, ΔH and entropy of adsorption, ΔS for the corrosion of mild steel in 1 M HCl in presence of GS was obtained by the equation:

$$CR = \frac{RT}{Nh} \exp\left(\frac{\Delta S}{R}\right) \exp\left(-\frac{\Delta H}{RT}\right) \tag{6}$$

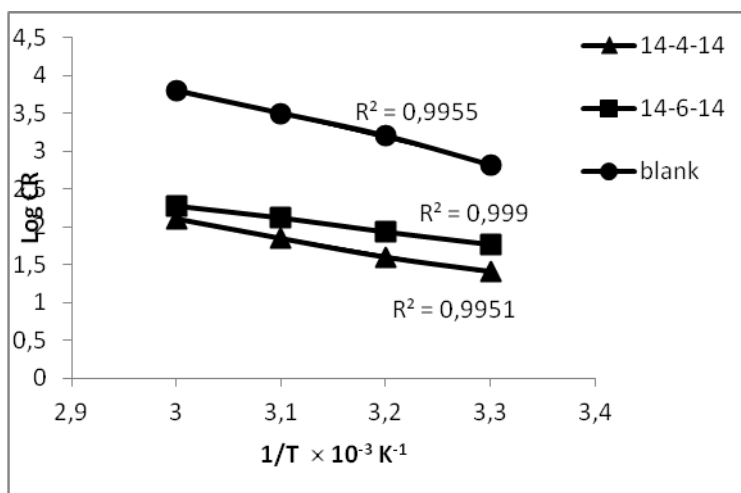


Figure 5. Log CR vs 1/T plots in absence and presence of surfactants.

Table 4. Calculated values of kinetic/thermodynamic parameters for mild steel in 1 M HCl in the absence and presence of GS from weight loss measurements.

Surfactants	E _a (kJ/mol)	ΔH (kJ/mol)	ΔS (kJ/mol ⁻¹ K ⁻¹)	Q (kJ/mol)	-ΔG _{ads} (kJ/mol)			
					30 °C	40 °C	50 °C	60 °C
BLANK	82.97	62.61	12.83	-	-	-	-	-
14-4-14	48.46	43.08	-77.18	21.25	44.82	35.24	37.79	40.11
14-6-14	35.33	31.02	-109.92	37.34	32.23	33.60	36.36	38.96

where, N is the Avogadro’s number, h is the Planck’s constant, R is the molar gas constant and T is the absolute temperature. Fig.6 shows the plots of log (CR/T) versus 1/T for blank and GS. Linear plot was obtained and from the slope $\left(-\frac{\Delta H}{2.303RT}\right)$ and intercept $\left[\log\left(\frac{R}{Nh}\right) + \left(\frac{\Delta S}{2.303R}\right)\right]$ of the linear plot, the values of ΔH and ΔS, respectively, were obtained. The calculated values of ΔH and ΔS are presented in Table 5. Considering the kinetic/ thermodynamic parameter for mild steel in 1M HCl in absence and presence of surfactants, the values of E_a and ΔH in presence of surfactants are lower than in absence of surfactants. This is due to decrease of the energy barrier of the corrosion reaction occurring at the steel surface. A change in the value of E_a in presence of surfactants may be due to the modification of the mechanism of the corrosion process in presence of adsorbed inhibitor molecules. In general, higher values of E_a in presence of additives support physical adsorption mechanism whereas an unchanged or lower value of E_a for inhibited systems compared to the blank is indicative of chemisorption mechanism. The inhibitor causing an increase in the values of E_a compared to blank retard the corrosion at ordinary temperature, but the inhibition is diminished at elevated temperature.

In the present investigation the value of E_a in presence of additives is lower compared to the blank and hence supports chemisorption mechanism.

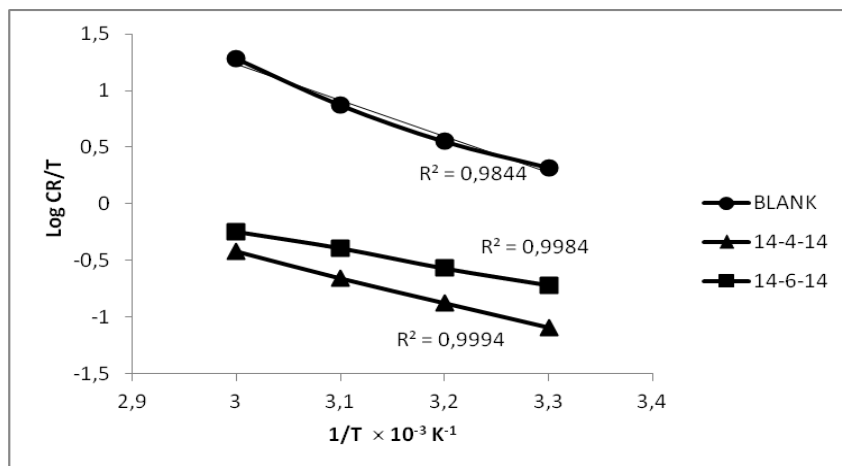


Figure 6. Log CR/T vs 1/T plots in the absence and presence of surfactants.

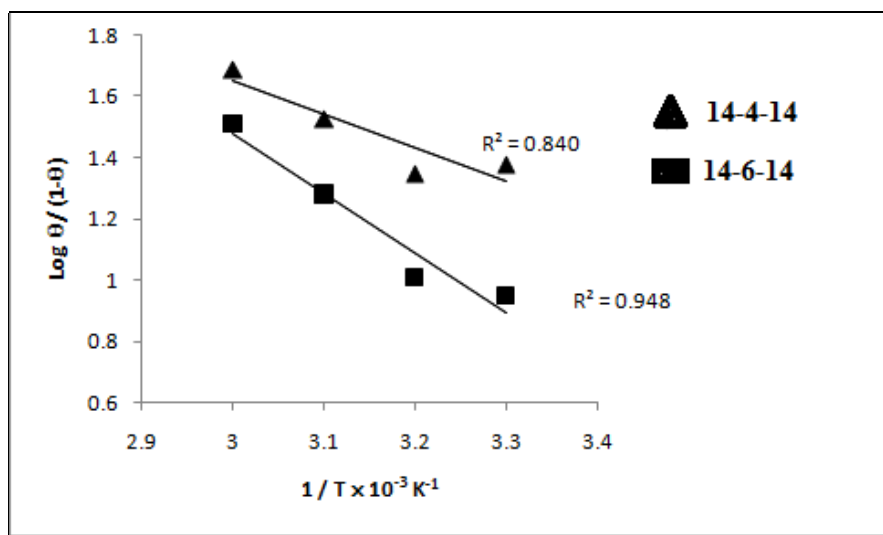


Figure 7. Log $(\theta/(1-\theta))$ vs 1/T plots in presence of surfactants.

The enthalpy of adsorption also decreases in presence of the GS compared to the free acid solution, this further support the mechanism of chemisorption. The values of ΔS are negative which indicates an increase in the system order in the presence of surfactants [37]. Fig.7 shows the plot of $\log \left(\frac{\theta}{1-\theta} \right)$ versus $1/T$ for the surfactants. From the slope $\left[\frac{-Q}{2.303R} \right]$ of the linear plot, heat of adsorption, Q_{ads} was obtained. The calculated values of Q_{ads} are positive (Table 5) indicating that the adsorption of GS on mild steel surface is endothermic. The free energy of adsorption, ΔG_{ads} is related to K_{ads} values with the following equation [38]:

$$K_{ads} = \frac{1}{55.55} \exp\left(-\frac{\Delta G_{ads}}{RT}\right) \quad (7)$$

The calculated values of ΔG_{ads} at 30-60°C for each GS are presented in Table 5. The negative values of ΔG_{ads} indicate the spontaneous adsorption of the GS on the mild steel surface. It is an established fact that values of ΔG_{ads} around -20 kJ mol^{-1} or less indicates physisorption. The values of ΔG_{ads} around -40 kJ mol^{-1} or more are considered as chemisorptions. However, the values of ΔG_{ads} between -20 and -40 kJ mol^{-1} gives a disputed Judgment about the type of adsorption [39, 40]. In the present investigation the values of ΔG_{ads} are between -30 and $-44.82 \text{ kJ mol}^{-1}$ suggesting a mixed type of adsorption involving both physisorption and chemisorption. However, the variation in the values of %IE with temperature and lower values of E_a and ΔH in presence of additives compared to blank suggest major contribution of chemisorption in the adsorption process.

3.5. Solution analysis of metal ion

The corrosion rate of mild steel in 1 M HCl in absence and presence of G.S at 30°C was also measured by determining the total iron ions entered into the test solution during the course of immersion and the result is shown in Table 5. The %IE obtained by solvent analysis is consistent with %IE determined by weight loss measurements

Table 5. Calculated values of corrosion rate and IE for mild steel in 1M HCl in absence and presence of GS at 30°C from weight loss measurement from solvent analysis of iron ions into test solution

Surfactant Concentration (M)	Corrosion rate ($\text{gm}^{-2} \text{ h}^{-1}$)	% Inhibition Efficiency (% IE)
Blank	1.76	-
14-4-14		
2.5×10^{-6}	0.27	84.66
5×10^{-6}	0.19	89.20
2.5×10^{-5}	0.08	95.63
14-6-14		
2.5×10^{-6}	0.65	63.07
5×10^{-6}	0.31	82.39
2.5×10^{-5}	0.15	91.48

3.6. Potentiodynamic polarization measurements

The potentiodynamic polarization curves for the corrosion of mild steel in 1M HCl solution in absence and presence of different concentration of surfactants are shown in Fig.8.

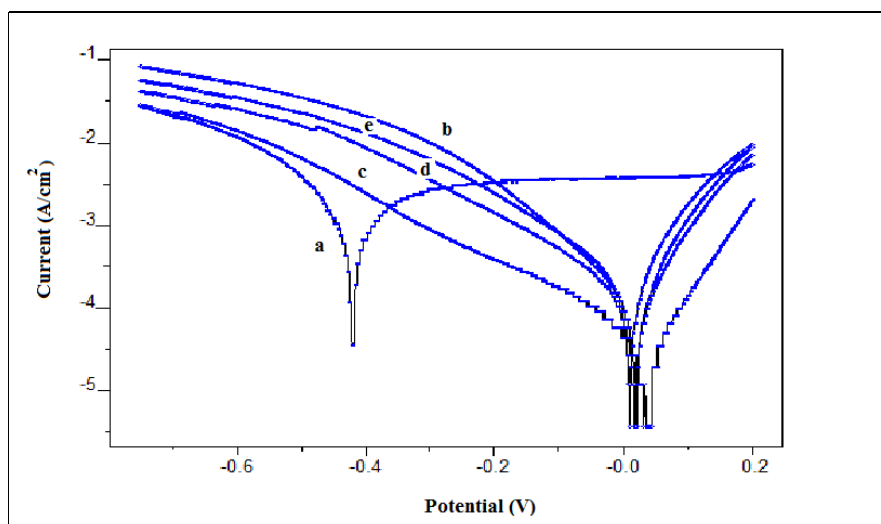


Figure 8. Potentiodynamic polarization curves for mild steel in 1 M HCl in absence and presence of different concentration of surfactants (a) Blank (b) 14-4-14 (2.5×10^{-5} M), (c) 14-4-14 (2.5×10^{-7} M), (d) 14-6-14 (2.5×10^{-5} M), (e) 14-6-14 (2.5×10^{-7} M).

The values of electrochemical parameters as deduced from these curves e.g., corrosion potential (E_{corr}) corrosion current density (i_{corr}), cathodic Tafel slope (β_c), anodic Tafel slope (β_a) and % IE are shown in Table 6. The IE was calculated by using the following equation:

$$\%IE = \frac{i_{corr}^o - i_{corr}}{i_{corr}^o} \times 100 \quad (8)$$

where, i_{corr}^o and i_{corr} are the corrosion current density in absence and presence of inhibitors, respectively. The study of electrochemical data reveals that the value of i_{corr} decreases in presence of additives, the decrease in i_{corr} is more pronounced at higher concentration of surfactants. The values of E_{corr} in presence of surfactants shift to more positive values compared to the blank, suggesting the dominant role of anodic suppression in the process [41]. The positive displacement in E_{corr} is more than 85mV suggesting that compounds acts as anodic type inhibitor [42,43]. There is a change in the values of both β_a and β_c indicating that the corrosion of mild steel in presence of surfactants is under both anodic and cathodic control. The values obtained from weight loss and electrochemical methods remain slightly different, this may be due to the fact that IE calculated from weight loss method is an average value, while the IE obtained from electrochemical method in an instantaneous value rather than an average value. The electrochemical results on the whole, are in good agreement with the weight loss results.

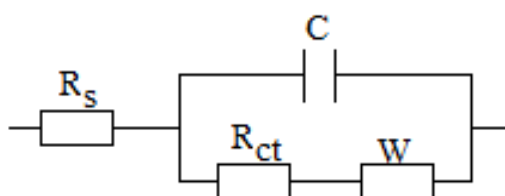
Table 6. Electrochemical parameters for corrosion of mild steel in 1 M HCl in the absence and presence of GS concentration at 30°C

Surfactant concentration (M)	E_{corr} (V)	$I_{corr} \times 10^{-3}$ (A/cm ²)	β_a (V/dec)	β_c (V/dec)	CR (mmpy)	%IE
BLANK	-0.439	3.03	5.005	0.286	9.914	-
14-4-14						
2.5×10^{-5}	0.045	0.032	0.086	0.236	0.103	98.9
2.5×10^{-7}	0.085	0.83	0.098	0.359	2.7	72.61
14-6-14						
2.5×10^{-5}	0.051	0.26	0.094	0.305	0.84	91.4
2.5×10^{-7}	0.053	0.65	0.109	0.359	2.12	78.5

3.7. EIS measurements

EIS diagrams for mild steel in 1M HCl obtained in absence and presences of GS are shown in Fig.9 and Fig.10. The phase angle at high frequencies provides a general idea of the anti corrosion performance of the inhibitors. The more negative the phase angle the more capacitive the electrochemical behavior [44]. Considering the appearance of phase angle vs. frequency diagrams Fig.9, the increase in surfactants concentration from 2.5×10^{-7} - 2.5×10^{-5} M results in more negative values of phase angle at high frequencies. This is indicative of superior inhibitive behavior of surfactants at high concentration. Further, the increase in surfactants concentration caused an increase in the absolute impedance at low frequencies in Bode plots. This is indicative of the enhanced adsorption of surfactants molecules on the mild steel surface. Figure 10 shows the typical fitting results of EIS diagram with the provided equivalent circuit where R_s represents solution resistance, R_{ct} charge transfer resistance, C the double layer capacitance and W , the Warburg resistance. The best fit parameters are shown in Table 7. The IE was obtained from the following equation.

$$\%IE = \frac{(R_{CT}^0 - R_{CT})}{R_{CT}^0} \times 100 \tag{9}$$



where, R_{ct}^0 and R_{ct} are the charged transfer resistance in absence and presence of surfactants, respectively. It is apparent that in presence of surfactants the value of R_{ct} increases whereas the value of C decreases. Further, the increase in surfactants concentration brings about an increase in the diameter of the semicircular capacitive loop. The increase in R_{ct} values in presence of surfactants is attributed to the formation of a protective film on the mild steel/HCl solution interface [45, 46]

Table 7. EIS parameters for corrosion of mild steel in 1M HCl in the absence and presence of gemini surfactants concentration at 30°C

Surfactant concentration (M)	R_s	R_{ct}	$C \times 10^{-5}$	W	%IE
BLANK	5.67	8.45	3.14	3×10^{-2}	-
14-4-14					
2.5×10^{-5}	22.2	131.6	1.81	-	93.58
2.5×10^{-7}	3.99	24.22	1.76	3.9×10^2	65.11
14-6-14					
2.5×10^{-5}	9.42	62.3	0.43	5.34	86.44
2.5×10^{-7}	5.7	1.86	2.46	5.99×10^{-1}	54.59

whereas, a decrease in C values is due to increase in the thickness of electrical double layer [47]. The further suggests that the investigated surfactants function by adsorption at the mild steel/ HCl solution interface leading to the formation of a protective film [48]. The IE as obtained by EIS measurements, in general, is consistent with the IE obtained by potentiodynamic polarization measurements.

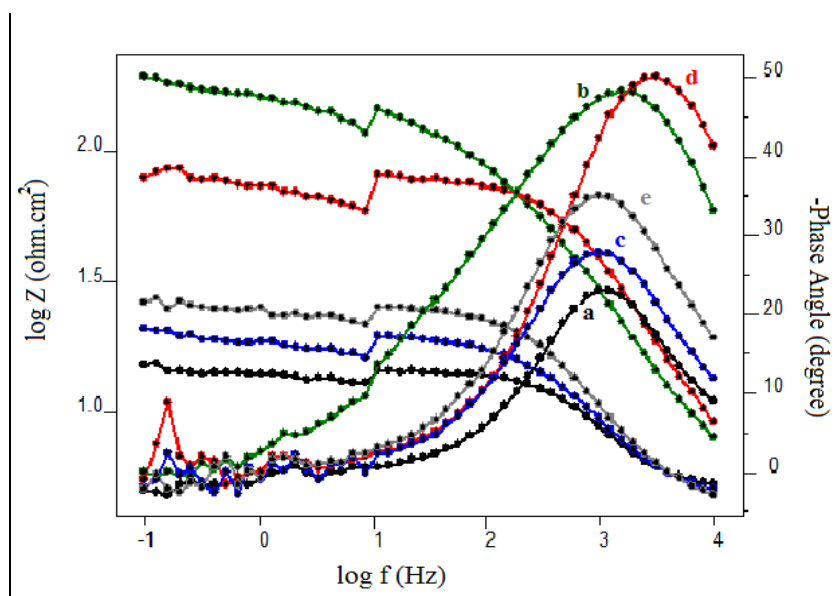


Figure 9. Bode diagrams of mild steel in 1 M HCl in absence and presence of different concentration of inhibitors (a) Blank (b)14-4-14 (2.5×10^{-5} M), (c) 14-4-14 (2.5×10^{-7} M), (d) 14-6-14 (2.5×10^{-5} M), (e) 14-6-14 (2.5×10^{-7} M).

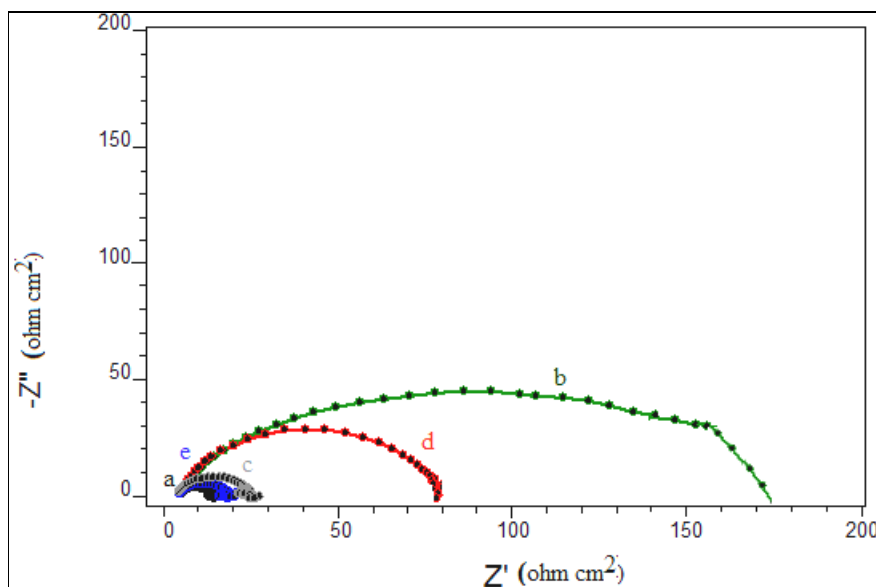
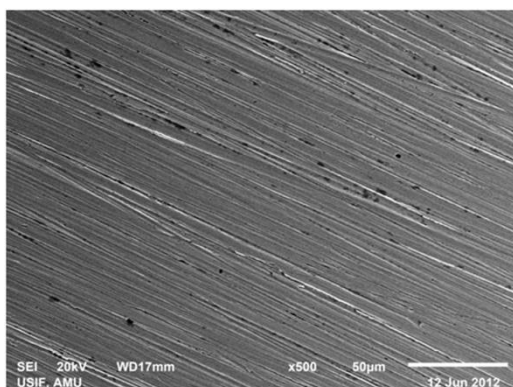


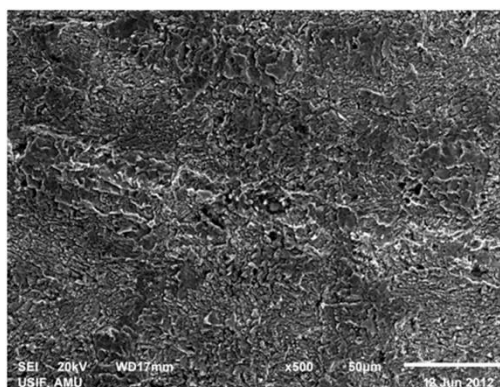
Figure 10. Comparison of experimental impedance measured for mild steel immersed in (a) Blank (b) 14-4-14 (2.5×10^{-5} M), (c) 14-4-14 (2.5×10^{-7} M), (d) 14-6-14 (2.5×10^{-5} M), (e) 14-6-14 (2.5×10^{-7} M).

3.8. SEM and AFM studies

SEM and AFM studies were carried out so as to determine if the mild steel corrosion inhibition is due to the formation of a protective film by adsorption of inhibitor. The SEM photomicrographs of the blank mild steel surface and steel surface exposed to uninhibited and inhibited acid solution are shown in Fig.11. The surface morphology of the blank mild steel sample shows a polished surface which is free from any noticeable defects such as cracks and pits. The marks on the surface are the streaks made during polishing with emery papers (Fig.11 a). In uninhibited acid solution (Fig. 11 b) a damaged and heterogeneous surface is observed. The surface heterogeneity is considerably decreased in the presence of surfactant additives (Fig.11 c and d). The decrease in the surface heterogeneity would have been caused by the deposition of the surfactants molecules on the mild steel surface which protected the surface from the attack of corrosive medium.



(a)



(b)

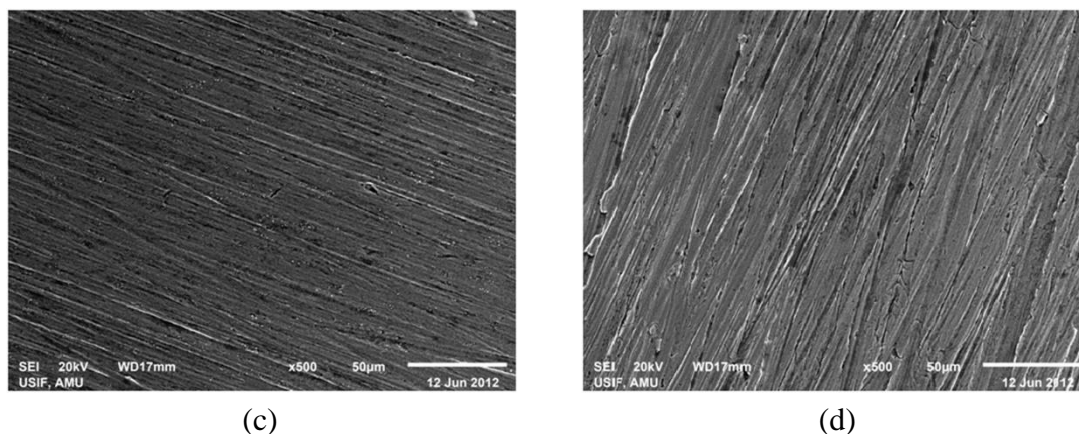
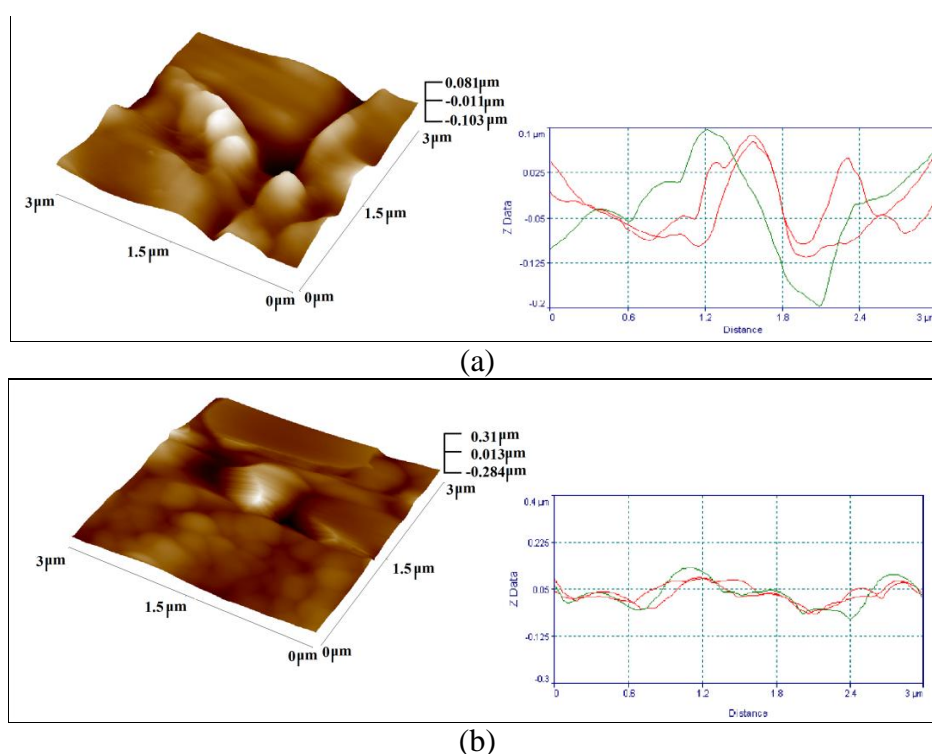


Figure 11. SEM pictographs of mild steel sample (a) Polished, (b) dipped in 1 M HCl, (c)dipped 14-6-14 (2.5×10^{-5} M),(d) dipped in 14-4-14 (2.5×10^{-5} M).

The SEM results are further proved by AFM photographs of blank mild steel surface and steel surface exposed to uninhibited and inhibited acid solution (Fig.12). The AFM photographs were taken at room temperature in the range of 0-3µm and 0-2µm, respectively. The average roughness of blank mild steel surface (Fig.12 a) is 0.081 µm which was found to be 0.333 µm in presence of uninhibited 1 M HCl solution (Fig.12 b). The cracks on the steel surface due to acid attack are clearly evident in the photograph. However, in presence of optimum concentration of 14-4-14 and 14-6-14 the average roughness was reduced to 0.165µm and 0.13µm, respectively (Fig. 12 c and 12 d). A smoother layer with clearly different morphology is as a result of the formation of a protective layer by the adsorbed inhibitor. The inhibitor layer is not very compact and as such does not provide absolute coverage, with some metal sites still exposed to acid attack.



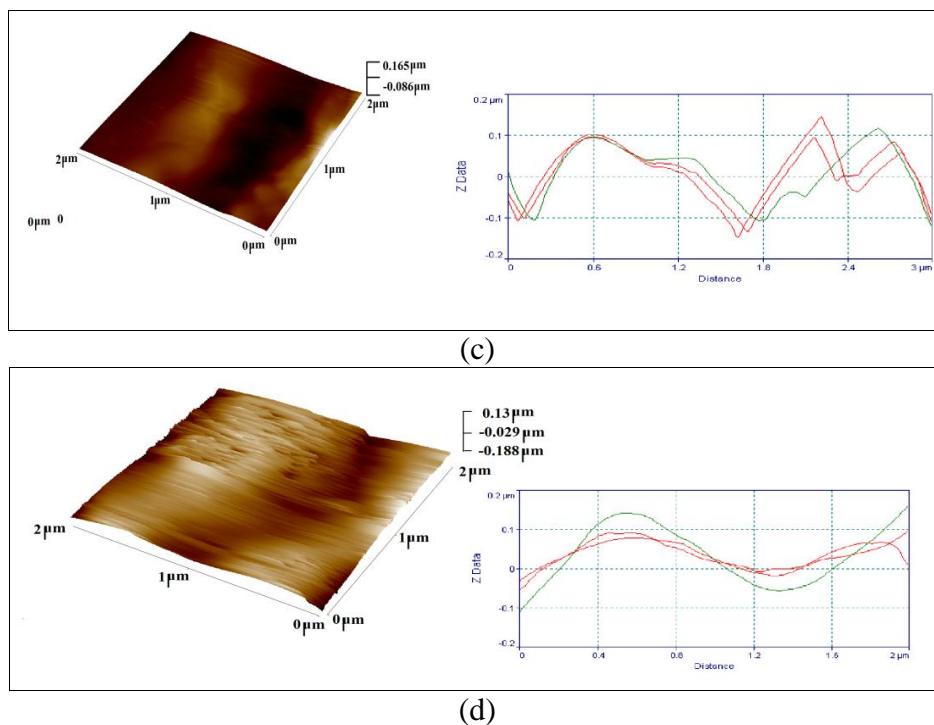


Figure 12 AFM photographs of mild steel sample (a) Polished, (b) dipped in 1 M HCl, (c) dipped in 14-6-14 (2.5×10^{-5} M), (d) dipped in 14-4-14 (2.5×10^{-5} M).

4. CONCLUSION

The cationic gemini surfactants showed good performance as corrosion inhibitor for mild steel in 1M HCl. The weight loss data suggest corrosion inhibition by adsorption mechanism and fits well to the Langmuir adsorption isotherm at various concentrations and temperatures studied. The phenomenon of chemical adsorption was followed from the trend of inhibition efficiency with temperature and values of E_a , ΔH and ΔG_{ads} . The results of potentiodynamic polarization measurements are consistent with the results EIS measurements. Gemini surfactants act as anodic type inhibitors. The SEM and AFM surface analysis showed smoother surface for steel in inhibited acid solution. The inhibition behavior is slightly affected by the spacer length of the surfactants, the surfactant 14-4-14 being more effective as an inhibitor for steel corrosion.

ACKNOWLEDGEMENTS

One of the authors (Sheerin Masroor) thankfully acknowledges the financial assistance from UGC, New Delhi for Maulana Azad National Fellowship.

References

1. Q. B. Zhang, Y.X. Hua, *Electrochimica Acta* 54 (2009) 1881-1887.
2. X.Li, L.Tang, L.Li, G.Mu, G.Liu, *Corros. Sci.* 48 (2006) 308.
3. M.Benabdellah, A.Aouniti, A.Dafalli, B.Hammouti, M.Benkaddour, A.Yahyi, A.Ettouhami, *Appl.Surf.Sci.*252 (2006) 8341.

4. K.C.Emregul, M.Hayvali, *Mater.Chem.Phys.* 83 (2004) 209.
5. G.Y.Elewady, *Int.J.Electrochem.Sci.* 3 (2008) 1149-1161.
6. M.Lebrini, M.Lagrene, H.Vezin, L.Gengembre, F.Bentiss, *Corros. Sci.* 47 (2005) .
7. F.Bentiss , M.Traisnel, N.Chaibi, B.Mernari, H.Vezin, M.Lagrene, *Corros. Sci.* 44 (2002) 2271.
8. S.Sayed , E.R.Abd, H.Hamdi, A.Hassan, A.Mohammed, *Mater. Chem .Phys.* 78 (2002) 337.
9. M.A.Quraishi, M.Z.A.Rafique, N.Saxena, S.Khan, *J.Corros.Sci. Eng.* 10 (2006).
10. M.A.Quraishi, F.A.Ansari, *J.Appl.Electrochem.* 36 (2006) 309.
11. M.Mobin , M.A.Khan & M.Parveen, *J.of Appl Polymer Science* , 121, (2011) 1558-1565.
12. M.Mobin, Mosarrat Parveen and M.Alam Khan, *Portugaliae Electrochimica Acta*, 29 (6) (2011) 391-403.
13. S.A.Umoren ,O.Ogbobe, P.C.okafor, E.E Ebenso , *J.Appl.Poly. Sci.* 105 (2007) 3363-3370.
14. D.Schweinsberg, G.George, A.Nanayakkawa and D.Steinert, *Corros. Sci.*, 28 (1988) 33.
15. F.Dabosi, Y.Derbali, M.Etman, A.Srhiri, A.de Savignac, *J.Appl.Electrochem.* 21 (1991) 225.
16. M.El Achouri, M.S. Hajji, S.Kertit, M.Essassi,M.Salem, R.Coudert , *Corros. Sci.* 37 (1995) 381.
17. T.Vasudevan, S.Muralidharan , S.Alwarappan, S.V.K.Iyer, *Corros. Sci.* 37 (1995) 1235.
18. El Achouri , M.,Hajji, M.S.,Salem, M.,Kertit, S.,Aride, J.,Coudert, R., and Essassi, E.M. *Corrosion* 52 (1996) 103-108.
19. Migahed, M.A., and Al-Sabagh, A.M, *Chem.Engg.Comm.*, 196 (2009), 1054-1075.
20. Free, M.L. *Corrosion* 58 (2002) , 1025-1030.
21. Saleh, M., Atia, A.A., *J.Appl.Electrochem.* 36 (2006) 899-905.
22. Wang, W. L., and Free, M. L. , *Corros.Sci.*, 46 (2004), 2601-2611.
23. Atia,A.A., and Saleh , M.M., *J.Appl.Electrochem.*, 33 (2003) 171-177.
24. Soror,T. Y., and El-Ziady, M.A., *Mater.Chem.Phys.*, 77 (2002) , 697-703.
25. Xueming, Li., Libin, Tang., Hongcheng, Lie., Guannan, Mu., and Guangheng, Lie., *Mater.Lett.*, 62 (2008) 2321-2324.
26. Y. Reyes, F.J. Rodriguez, J.M. del Rio, M. Corea, F. Vazquez, *Progress in Organic Coating* 52 (2005) 366.
27. M.El.Achouri, S.Kertit, H.M.Gouytaya, B.Nciri, Y.Bensouda, L.Perez ,M.R.Infante, K.Elzacemi, *Progress in Organic Coating* 43 (2001) 267-273.
28. F. A. Ansari, M.A. Quraishi, *Portugaliae Electrochim Acta* 28(5)(2010)321.
29. H. K. Sharma, M.A. Quraishi, *Indian J. Chem. Tech.* 14(2007) 494.
30. F. A. Ansari, M.A. Quraishi, *Arabian J. Sci. Eng.* 36 (2011)11.
31. L.G. Qui, A.J. Xie, Y.H. Shen, *Mater. Chem. Phys.* 87 (2004) 237.
32. S.De, V. K. Aswal, P.S. Goyal, S. Bhattacharya, *J. Phys. Chem.* 100 (1996) 11664
33. Kabir-ud-Din, W. Fatma, Z. A. Khan, *Colloid Polym. Sci.* 284 (2006) 1339.
34. R.Vera., R.Schreble, P. Cury ., R.Del Rio., H.Romero., *J.Applied.Electrochem.* 37 (2007) 519-529.
35. R.Ansar ., A.H.Alikhani., *J.Coat.Tech.Res.*, 6(2) (2009) 221-227.
36. W.Huang and J.Zhao, *Colloids and Surface.A: Physicochem Eng Aspects*, 278(2006) 246.
37. A.Frignani, M.Tassinari, L.Meszáros, G.Trabanelli, *Corrosion Sci.*, 32 (1991) 903.
38. E.Khamis, *Corrosion* . 46 (1990) 476.
39. De Souza, F.S., and Spinelli, A., *Corros.Sci.*, 51(3) (2009) 642-649.
40. Li, W.H., He, Q., Zhang, S.T., Pei, C.L and Hou, B.R., *J.Appl.Electrochem* 38 (3) (2008) 289-295.
41. Hu, L., Zhang, S., Li, W., Hou, B., *Corrosion Sci.*, 52 (2010) 2891.
42. Riggs, O.L., *Corrosion*, 31 (1975) 128.
43. E.S Ferriera, C.Giancomelli, F.C.Giacomelli and A.Spinelli, *Mater. Chem. Phys.*, 83 (2004) 129.
44. M.Mahdavian, S.Ashhari, *Electrochimica Acta* 55 (2010) 1720-1724.
45. F.Bentiss , M.Traisnel and M.Lagrene, *Corrosion . Sci.*, 42 (2000) 127.
46. S.Murlidharan, K.L.N.Phani, S.Pitchumani and S.Ravichandaran, *J.Electrochem.Soc.*, 142 (1995) 1478.
47. M.G.Hosseini, M.Ehtisham Zadeh and T.Shahrabi, *Electrochem.Acta*, 52 (2007) 3680.

48. M.Bouklah, B.Hammouti, A.Aouniti, M.Benkaddour and A.Bouyanzer, *Appl.Surf.Sci.*, 252 (2006) 6236.